Nuclearity and cooperativity effects in binuclear catalysts and cocatalysts for olefin polymerization

Hongbo Li and Tobin J. Marks*

Department of Chemistry, Northwestern University, Evanston, IL 60208-3113

Edited by Jack Halpern, University of Chicago, Chicago, IL, and approved June 15, 2006 (received for review April 26, 2006)

A series of bimetallic organo-group 4 "constrained geometry" catalysts and binuclear bisborane and bisborate cocatalysts have been synthesized to probe catalyst center–catalyst center cooperativity effects on olefin enchainment in homogenous olefin polymerization and copolymerization processes. Significant nuclearity effects are found versus mononuclear controls, and the effect can be correlated with metal–metal approach distances and ion pairing effects. Novel polymer structures can be obtained by using such binuclear catalyst/cocatalyst systems.

catalysis | polymer | polyolefin

Enzymes achieve superior reactivity and selectivity, in part, by their efficacy in creating high local reagent concentrations and special, conformationally advantageous active site–substrate proximities and interactions (1–4). In this regard, the possibility of unique and more efficient abiotic catalytic transformations based on cooperative effects between adjacent active centers in multinuclear transition metal complexes is currently of great interest. Within the context of the rapidly advancing and technologically significant field of homogeneous single-site olefin polymerization catalysis (5–10), the conjecture that cooperative effects involving two or more metal centers in close proximity might achieve more efficient chain propagation and/or novel polymer architectures motivated the research that is the subject of this contribution.

Single-Site Olefin Polymerization Processes

One of the most exciting developments in the areas of catalysis, organometallic chemistry, and polymer science in recent years has been the intense development of new polymerization technologies based on well defined single-site metallocene and coordination complex olefin polymerization catalysts (5–10). The active catalytic species is typically generated by combining a transition-metal organometallic precursor with an activator or cocatalyst. The resulting electrophilic/coordinatively unsaturated, strongly ion-paired species then undergoes rapid olefin enchainment. In optimum cases (e.g., group 4 metal and cyclopentadienyl-type ligand), catalysts with truly exceptional productivities and selectivities for high-molecular-weight polyolefins are produced.

Constrained Geometry Catalysts: Testbeds for Multinuclear Cooperativity Effects

Group 4 "constrained geometry" catalysts (CGCs) (**A**; Fig. 1) are well known single-site polymerization agents (16, 17) that produce unusual branched, hence far more processable, polyethylenes with high productivity and selectivity. One of the key features of these catalysts is the coordinatively open nature of the active site, which allows rapid enchainment of sterically encumbered olefin comonomers into the polyethylene backbone. Under certain conditions, these catalysts yield vinyl-terminated, chain-transferred macromonomers (a macromolecule that acts as a monomer) that diffuse away and then undergo competitive reinsertion into a growing polymer chain to produce macromolecules with long chain branching (Fig. 19, which is published as supporting information on the PNAS web site). Compared with conventional metallocene catalysts, CGCs exhibit increased thermal stability and generally yield higher-molecular-weight polymers (18). Given these unique CGC properties, the intriguing question then arises as to whether, if two CGC centers could be held in sufficiently close spatial proximity and in proper mutual orientations, cooperative effects between the two unsaturated metal centers might exert a significant influence on the course of ethylene polymerizations and copolymerizations.

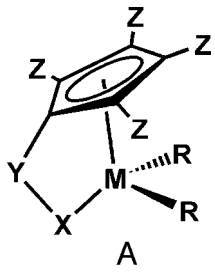

Fig. 1. Generalized structural motif for constrained geometry polymerization catalysts.

To this end, several families of binuclear CGC structures and analogous mononuclear control catalysts were synthesized (Fig. 2) (14–19). These complexes were accessed via a protodeamination protocol by using the mono- or bifunctional $CGCH_2$ ligands and driven to completion by continuous removal of the volatile $HNMe_2$ coproduct (Fig. 3) (14).

The subsequent reaction of the resulting mono- or bimetallic dimethylamido complexes with excess $AlMe_3$ at room temperature cleanly affords the corresponding dimethyl complexes. Methylene bridged **C1–Zr$_2$** and **C1–Ti$_2$** (15) require longer reaction times in the metallation step versus the $-CH_2CH_2-$ bridged analogue, presumably owing to steric constraints. In a similar manner, heterobimetallic catalyst **Ti$_1$Zr$_1$** can also be synthesized via multistep protodeamination and $AlMe_3$ alkylation pathways (19). The first step is the formation of a monometallic amido complex via reaction of the free ligand with 1.0 eq of $Zr(NMe_2)_4$. This intermediate product is then subjected to reaction with 1.0 eq of $Ti(NMe_2)_4$ to obtain the heterobimetallic amido complex **Ti$_1$Zr$_1$(NMe$_2$)$_4$**. The sequence of first introducing $Zr(NMe_2)_2$ then $Ti(NMe_2)_2$ is used because the former ligand substitution process is far more rapid and more selective. For control experiments, monometallic CGC complexes **Zr$_1$** and **Ti$_1$** were synthesized via methodologies similar to those for the bimetallic complexes (14, 17) (Fig. 20, which is published as supporting information on the PNAS web site).

Selected crystal structures of bimetallic CGCZr complexes are shown in Figs. 4 and 5. Fig. 4 shows the solid-state structure of bimetallic bis(dimethylamido) Zr complex EBICGC$[Zr(NMe_2)_2]_2$ (EBI = ethylenebisindenyl), the precursor to **Zr$_2$** (14). The data

Conflict of interest statement: No conflicts declared.

This article is a PNAS direct submission.

Abbreviation: CGC, constrained geometry catalyst.

*To whom correspondence should be addressed. E-mail: t-marks@northwestern.edu.

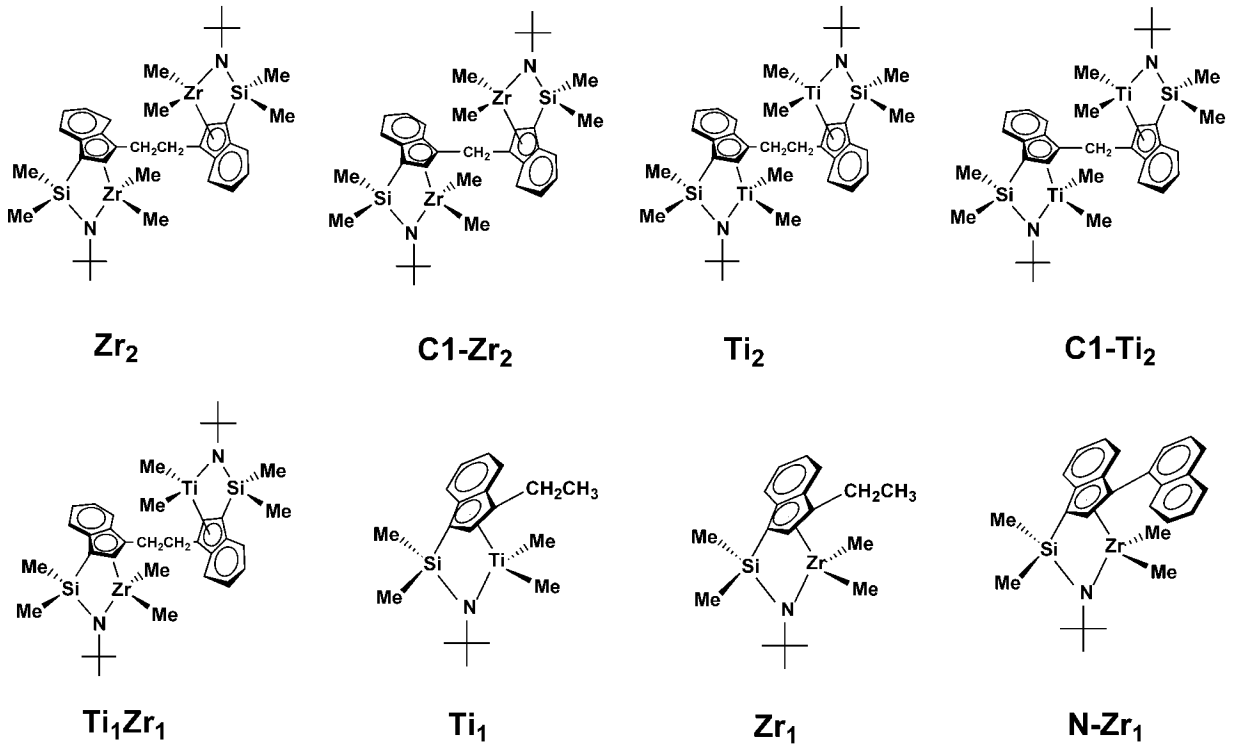

Fig. 2. Binuclear and mononuclear constrained geometry catalysts and compound labeling scheme.

reveal an inversion center with a CGCM< unit located on either side of the $-CH_2CH_2-$ bridge ligand framework with the π-coordinated indenyl rings in a diastereomeric relationship. Similar catalyst structures are observed for binuclear catalysts EBICGC $[Ti(NMe_2)_2]_2$ and EBICGC$[Ti(NMe_2)_2][Zr(NMe_2)_2]$. In contrast, small variations in the ligand bridge structure can lead to dramatic changes in catalyst conformation. Fig. 5 shows the *methylene*-bridged bimetallic bis(dimethylamido) Zr complex MBIC GC$[Zr(NMe_2)_2]_2$, which has an asymmetric structure with a large computed barrier (≈65 kcal/mol) to rotation about the ring–CH_2–ring bridging connections; in contrast, the computed barrier for the ring–CH_2CH_2–ring catalysts is negligible. It can be seen that the shorter methylene bridge forces the two indenyl rings into a twisted conformation. This locates the two Zr centers to the same side of the molecule, in a significantly different disposition than that in the structure of EBICGC$[Zr(NMe_2)_2]_2$. Such structural differences lead to significantly different catalytic behavior, as will be discussed below.

Binuclear Perfluorophenyl Bisborane and Bisborate Cocatalyst Syntheses, Structures, and Catalyst–Cocatalyst Ion-Pairing

The processes which transform organo-group 4 complexes into active olefin polymerization catalysts almost invariably involve reagents (activators/cocatalysts) that create highly electrophilic, coordinatively unsaturated species via either protonolysis, alkide abstraction, or oxidative heterolysis. The activator/cocatalyst, which becomes an anion after the activation process, is a vital part of the catalytically active cation–anion ion pair and can significantly influence catalytic activity, stability, polymerization kinetic profile, and polymer molecular weight and stereo-regularity.

It will be seen that binuclear cocatalysts display important nuclearity effects in single-site polymerizations. A variety of binuclear cocatalysts have been synthesized, several of which are shown in Fig. 6 (14, 17, 20–22). For the synthesis of bisborane $\mathbf{BN_2}$, the metathesis of fluoroaryl tin reagents with a perfluorophenylborane precursor has proven to be an effective and general approach to synthesizing binuclear bisborane cocatalysts, as shown in Fig. 7 (15). As judged by ^1H and ^{19}F NMR spectroscopy, alkyl/chloride exchange occurs initially to afford 2.0 eq of $(C_6F_5)_2BMe$ and 1,4-$C_6F_4(SnMe_2Cl)_2$; the latter then undergoes reaction with the additional $(C_6F_5)_2BCl$ to yield 1,4-$(C_6F_5)_2BC_6F_4B(C_6F_5)_2$ ($\mathbf{BN_2}$) and 2.0 eq of Me_2SnCl_2.

A different type of binuclear cocatalyst, trityl bisborate $(Ph_3C^+)_2[1,4\text{-}(C_6F_5)_3BC_6F_4B(C_6F_5)_3]^{2-}$ ($\mathbf{B_2}$; Fig. 6), is derived

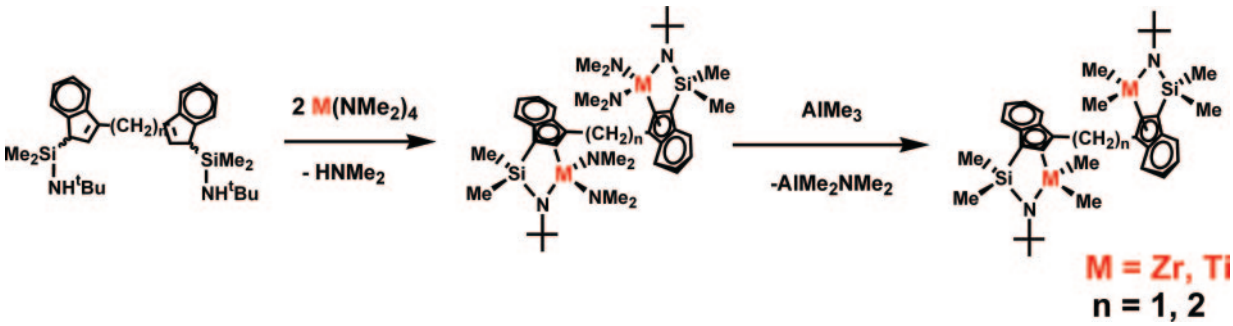

Fig. 3. Synthetic routes to binuclear CGCs.

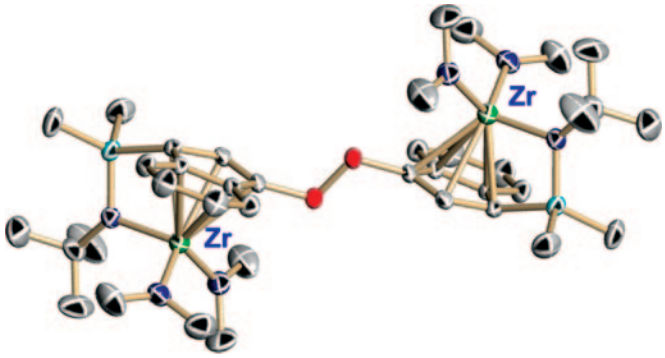

Fig. 4. Molecular structure of ethylene-bridged EBICGC[$Zr(NMe_2)_2]_2$. Thermal ellipsoids are drawn at the 50% probability level. A single enantiomer is shown for each complex.

from bisborane 1,4-$Br_2BC_6F_4BBr_2$ with 6 eq of C_6F_5Li (generated *in situ*) affords the dilithium bisborate salt $(Li^+)_2$[1,4-$(C_6F_5)_3BC_6F_4B(C_6F_5)_3]^{2-}$, which then undergoes subsequent cation metathesis with Ph_3CCl to yield bistrityl bisborate salt $\mathbf{B_2}$ (Fig. 21, which is published as supporting information on the PNAS web site).

Catalyst–cocatalyst ion pairs can be straightforwardly prepared from the corresponding catalyst and cocatalyst reagents having similar or different nuclearities. As an example of a mononuclear catalyst/cocatalyst ion pair, Fig. 8 shows the representative molecular structure of the activated organotitanium ion pair [1-Me_2Si-(3-ethylindenyl)(^{t}BuN)]$TiMe^+MeB(C_6F_5)_3^-$ (15). The Ti–Me(terminal) distance [2.090(3) Å] is 0.01–0.02 Å shorter than the Ti–Me distances in the neutral organotitanium precursor $\mathbf{Ti_1}$ [2.102(2) and 2.1100(2) Å] due to the increased metal electrophilic character, whereas the Ti–Me(bridging) separation is 0.230 Å longer, reflecting the largely ionic character of the ion pair interaction. NMR spectroscopy reveals characteristic fingerprints of a very coordinatively unsaturated, electrophilic metal center, as well as strong but coordinatively flexible ion pairing and negligible ion pair aggregation in the concentration ranges used for typical polymerization (23, 24).

Regarding multinuclear systems, reaction of $\mathbf{BN_2}$ with 2.0 eq of $(C_5H_5)_2ZrMe_2$ results in clean, instantaneous formation of the bimetallic ion pair $[(C_5H_5)_2ZrMe^+]_2${$Me_2$1,4-$C_6F_4[B(C_6F_5)_2]_2$}$^{2-}$ (15) (Fig. 22, which is published as supporting information on the PNAS web site). This result argues that any intermediate borate abstraction product resulting from reaction of the bisborane with 1.0 eq of $(C_5H_5)_2ZrMe_2$ is sufficiently Lewis acidic to abstract a methide anion from a second neutral metallocene dialkyl. The

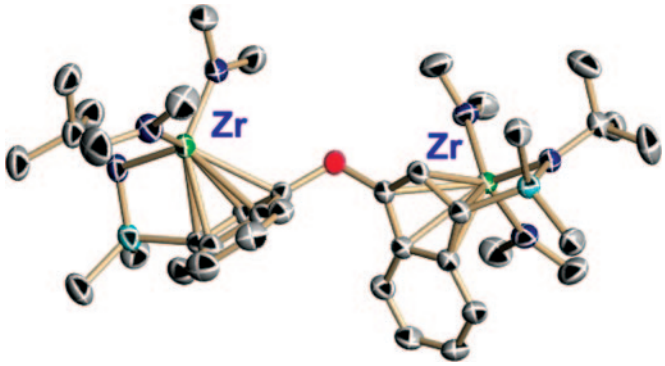

Fig. 5. Molecular structures of methylene-bridged MBICGC[$Zr(NMe_2)_2]_2$. Thermal ellipsoids are drawn at the 50% probability level. A single enantiomer is shown for each complex.

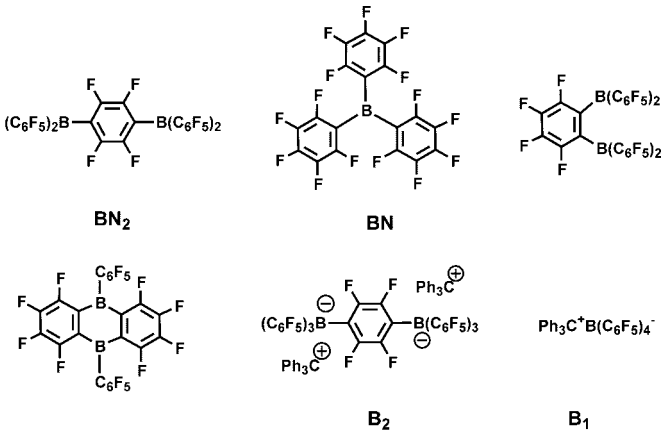

Fig. 6. Mononuclear and binuclear bisborane and bisborate cocatalysts.

crystal structure of the activated bimetallic complex $[(C_5H_5)_2ZrMe^+]_2${$Me_2$1,4-$C_6F_4[B(C_6F_5)_2]_2$}$^{2-}$ is shown in Fig. 9. The two zirconocenium cations are centrosymmetrically disposed on opposite sides of the arene plane, presumably reflecting repulsive steric and electrostatic interactions. It will be seen that binuclear catalyst/cocatalyst combinations display marked cooperative effects in homogenous olefin polymerization processes leading to unusual monomer/comonomer enchainment selectivities and unusual polyolefin architectures.

Binuclear Structures and Macromolecular Branch Formation in Ethylene Homopolymerization Processes

Linear low-density polyethylene (LLDPE)—long chain polyethylene with small but significant levels of C_4–C_6 alkyl branching—has excellent processability and high melt tension properties suitable for film manufacture (25, 26). Typically, linear low-density polyethylene branching is achieved via copolymerization of ethylene with a linear α-olefin comonomer. Single-site CGCs represent another major advance in this field, because the polyethylene produced also contains long-chain branches arising from competing intermolecular macromonomer re-enchainment as discussed above. Homogeneous "tandem catalysis" has also received attention as an alternative approach to branched polyethylenes. Here, a single-site catalytic center produces α-olefin oligomers, which are subsequently incorporated, via an intermolecular process, into high-molecular-weight polyethylene by a second, different single-site catalytic center present in the same reaction medium and using the same ethylene feed (26–28). It should be evident that, at typical polymerization concentrations, these intermolecular tandem processes are inherently inefficient. For these reasons, the attractive possibility of constraining two catalyst centers in close spatial proximity offers the potential for significantly enhanced macromonomer capture efficiency.

The effects of catalyst and cocatalyst nuclearity on the course of ethylene homopolymerizations can be probed systematically via the nuclearity matrix shown in Fig. 10 as well as by change in group 4 metal. For example, experimental traversal of a CGC organozirconium matrix (19) reveals that high effective local active-site concentrations and catalyst center–catalyst center cooperative effects are operative by bringing the electrophilic species into proximity via covalent and/or electrostatic bonding. For ethylene homopolymerization at constant conversion, the branch content of the polyolefin products, primarily ethyl branches, is significantly enhanced as the catalyst or cocatalyst nuclearity is increased. Compared with the catalyst derived from mononuclear $\mathbf{Zr_1}$ + $\mathbf{B_1}$, the catalyst derived from bimetallic $\mathbf{Zr_2}$ + bifunctional $\mathbf{B_2}$ produces ≈11 times more ethyl branches (predominant type of branch) in ethylene homopolymerization (Fig. 23, which is published as sup-

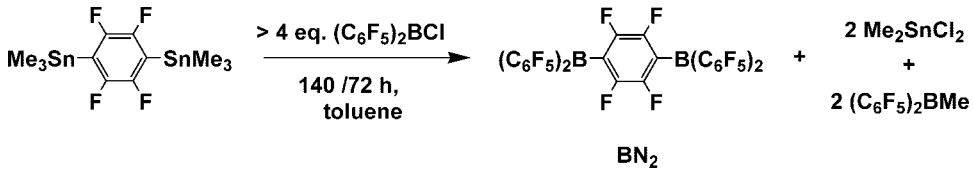

Fig. 7. Synthetic pathway to binuclear bisborane cocatalyst $\mathbf{BN_2}$.

porting information on the PNAS web site) via a process that is predominantly intradimer in character, as shown in Fig. 11. In this scenario, the eliminated oligomeric or polymeric vinyl macromonomer chain produced at one catalytic center is detained by *binuclear interactions* (presumably C–H···M^+ agostic interactions between the electrophilic metal center and electron-rich C–H bonds—the importance of mononuclear agostic examples is of course well established in cationic d^0 polymerizations (29–31), involving the adjacent electrophilic metal center, and the weakly bound oligomeric/polymeric α-olefinic fragment therefore has an enhanced probability of subsequent intramolecular re-enchainment with 1,2 regiochemistry at a proximate Zr-ethyl$^+$ or Zr-P$'^+$ site. This model is consistent with an observed increase in product molecular weight with increasing catalyst/cocatalyst nuclearity, with conversion-dependent experiments revealing significant quantities of ethyl branches (but few other branches) produced in the $\mathbf{Zr_2}$ + $\mathbf{B_2}$ polymerization system, even in the very earliest stages of the polymerization.

The methylene-bridged binuclear "constrained geometry catalyst" $\mathbf{C1–Zr_2}$ was used to further explore the Zr···Zr spatial proximity effects in bimetallic catalyst systems (16). Various cocatalysts and ion pair-weakening solvents were also examined to better understand the function of the binuclear catalyst systems. It is found that in ethylene homopolymerization with conventional cocatalysts, ≈70-times increases in molecular weight are achieved with $\mathbf{C1–Zr_2}$ vs. $\mathbf{C2–Zr_2}$ under identical polymerization conditions. Also with methylalumoxane as the cocatalyst, ≈600-times increases in polyethylene molecular weight are achieved with binuclear $\mathbf{C2–Zr_2Cl_4}$ and $\mathbf{C1–Zr_2Cl_4}$ vs. mononuclear $\mathbf{Zr_1Cl_2}$. Interestingly, when polar C_6H_5Cl is used as the polymerization medium, thereby weakening the catalyst–cocatalyst ion pairing, substantial alterations in catalyst response and polymer product properties are observed. Mononuclear vs. binuclear differences in activity and product molecular weight fall substantially. These results argue that achievable Zr···Zr spatial proximity, as modulated by the ion pairing, significantly influences chain transfer rates, and that such proximity effects are highly cocatalyst- and solvent-sensitive.

The significantly enhanced polymer product molecular weights in the $\mathbf{C1–Zr_2}$- vs.$\mathbf{C2–Zr_2}$-mediated polymerizations, and the relative activities of the two catalysts, suggest that chain termination rates are substantially depressed for $\mathbf{C1–Zr_2}$. These effects may reflect access to bridged structures in which proximate metal centers can coordinate/stabilize growing polymer chains, probably via agostic interactions (e.g., **B**; Fig. 12) (34–36), thereby impeding chain transfer to monomer and subsequent macromonomer dissociation as chain termination pathways, thus significantly reducing the overall chain termination rate. Different cocatalysts can also have a significant influence on competing chain termination pathways, hence yield different polymer architectures. Thus, as noted above, dramatically increased molecular weights are observed in binuclear CGCZr catalysts vs. mononuclear ones when methylalumoxane is used as the cocatalyst. *In situ* NMR studies of the ion pairs reveals that the two Zr centers can attain close proximity in bimetallic catalysts, indicated by the spectroscopic signatures of Zr-μCH_3-Zr species when bulky methylalumoxane is used as cocatalyst, thus suggesting possible structures to modulate chain termination pathways.

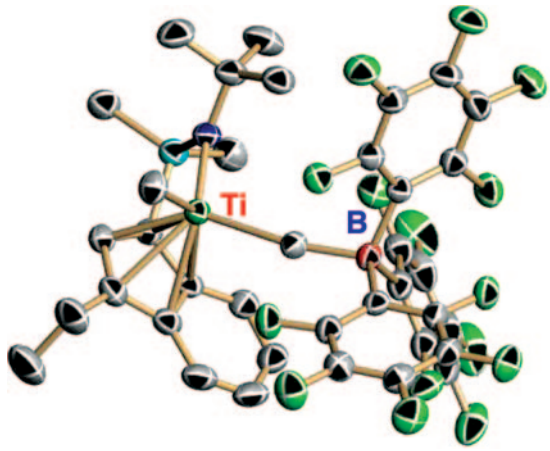

Fig. 8. Molecular structure of the mononuclear ion pair [1-Me_2Si(3-ethylindenyl)(^{t}BuN)]TiMe$^+$MeB(C_6F_5)$_3^-$. Thermal ellipsoids are drawn at the 50% probability level.

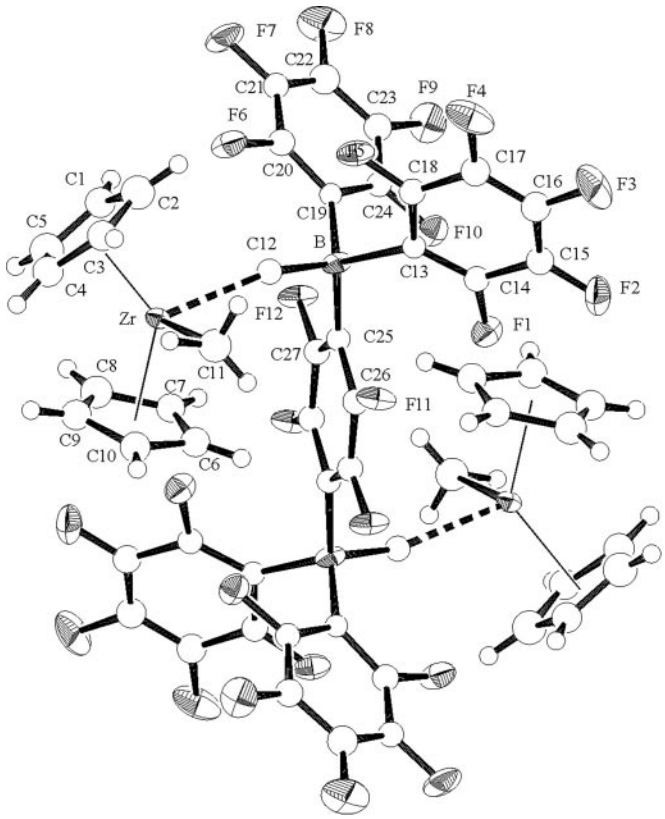

Fig. 9. Molecular structure and atom numbering scheme for $[(C_5H_5)_2ZrMe^+]_2\{Me_21,4C_6F_4[B(C_6F_5)_2]_2\}^{2-}$. Thermal ellipsoids are drawn at the 50% probability level.

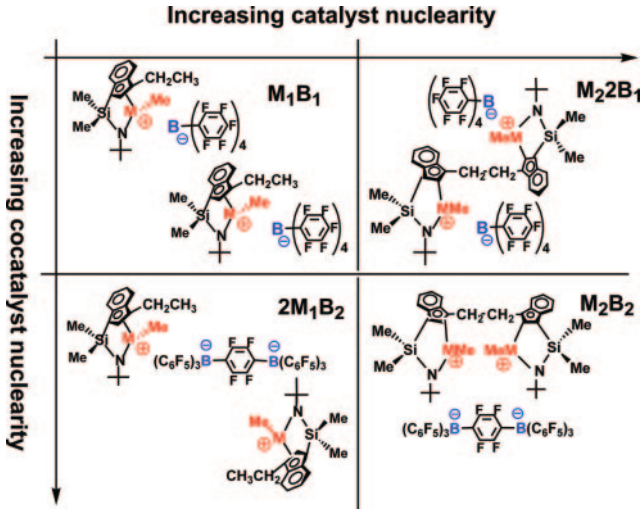

Fig. 10. Catalyst/cocatalyst nuclearity matrix for group 4 CGC-type catalysts.

Although the aforementioned binuclear organozirconium CGCs can achieve high levels of branching in olefin polymerization via what are clearly unusual enchainment pathways, CGCZr catalysts typically exhibit modest activities and do not generally produce high-molecular-weight polymers. In contrast, mononuclear CGCTi catalysts are known to afford high-molecular-weight polyolefins with high activity and high α-olefin co-enchainment efficiencies (11, 12). For this reason, nuclearity effects in the Ti system were of great interest. In a first investigation (32), marked cooperative effects were observed in *electrostatically joined* binuclear catalyst/cocatalyst combinations by using binuclear activator/cocatalyst counterdianion $\mathbf{B_2}$ to spatially confine heteronuclear pairs of mononuclear cationic centers, in which $\mathbf{Zr_1}$ was used as the source of vinyl-terminated ethylene oligomers and $Me_2Si(^tBuN)(\eta^5\text{-}C_5Me_4)TiMe_2$ (**Ti**) was used as the source of high-molecular-weight polymer because of its aforementioned ability to efficiently co-enchain α-olefins (Fig. 13) (11). It was found (32) that the use of $\mathbf{B_2}$ in ethylene polymerizations with stoichiometrically appropriate ratios of **Zr** and **Ti** catalysts (to suppress the probability of Ti···Ti pairs; Zr_1···Zr_1 yields small quantities of readily separated low-molecular-weight products) produces a *significantly* more homogenous polyethylene than that produced by the analogous polymerizations with $\mathbf{B_1}$ as the counteranion/cocatalyst (Fig. 14). The thermal and spectroscopic properties of the $\mathbf{B_2}$-derived polymer are consistent with relatively homogeneous, highly branched polyethylene, whereas $\mathbf{B_1}$ produces a heterogeneous mixture of high- and low-molecular-weight products. These results show that the binuclear bisborate activator $\mathbf{B_2}$ dramatically increases the efficiency of heterobimetallic olefin enchainment processes using the homogeneous **Ti** and **Zr** catalysts for linear low-density polyethylene synthesis. However, although these electrostatic effects clearly accentuate the unique characteristics of the component heteronuclear pairs (M_1, M_2; by manipulating relative concentrations and activities), they cannot exclusively select for them over other coexisting statistical components (M_1,M_1 + M_2,M_2).

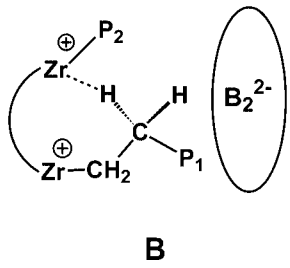

Fig. 12. Possible agostic C–H bonding interactions in bimetallic catalysts.

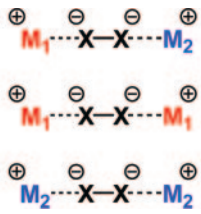

[1]

In an effort to fully exploit the potential of heteronuclear intramolecular cooperative effects, a new heterobinuclear com-

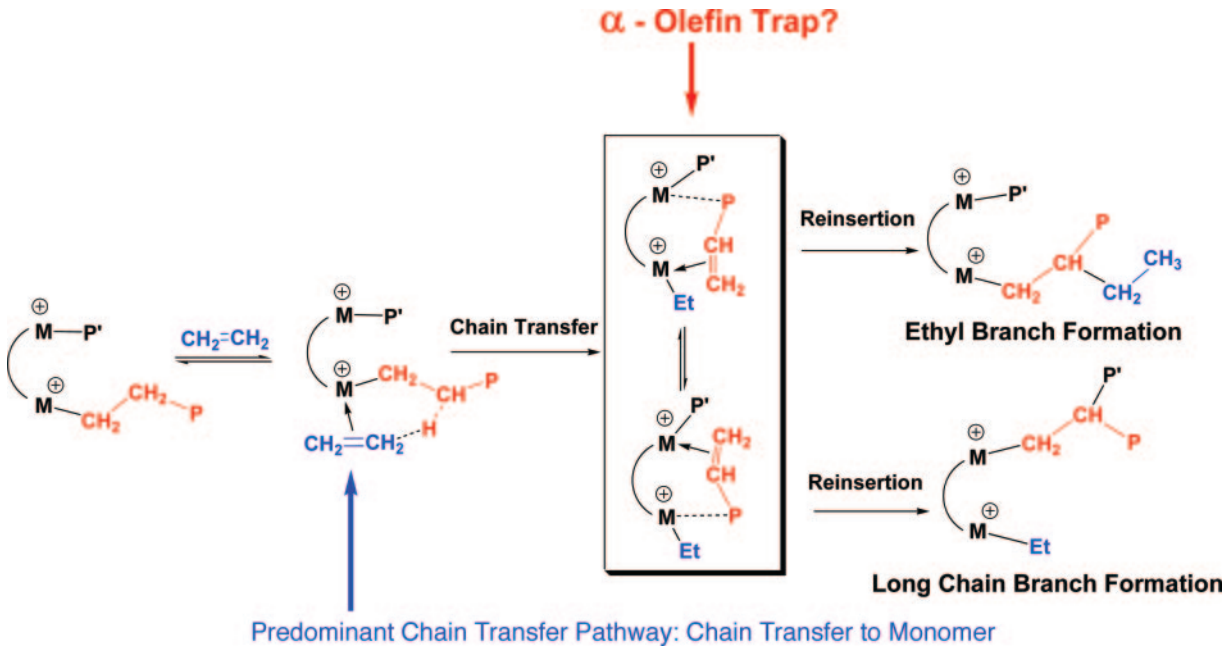

Fig. 11. Proposed pathways for branch formation facilitated by binuclear group 4 CGCs. P,P′ = polymeryl fragment.

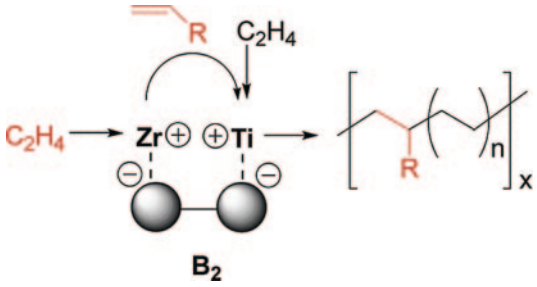

Fig. 13. Branch formation via B_2 activated electrostatically organized heterobimetallic group 4 catalysts.

plex, Ti_1Zr_1 (Fig. 24, which is published as supporting information on the PNAS web site) that *covalently links* ZrCGC and TiCGC moieties was synthesized (Fig. 15) (19). Here, the monometallic Ti center is expected to produce high-molecular-weight polyethylenes with high activity, whereas a mononuclear Zr center should produce with moderate activity low-molecular-weight polyethylenes having reactive vinylic end groups. Such catalysts can exclusively hold one Zr and one Ti center in proximity, thus enhancing the enchainment selectivity for branch formation. Indeed, the polymerization results reveal that catalyst Ti_1Zr_1 is competent to produce long-chain ($\geq C_6$) branched polyethylenes in ethylene homopolymerization processes with high selectivity and efficiency (19).

Binuclear Catalytic Cooperative Effects in Ethylene + α-Olefin Copolymerizations

Significant binuclear effects are also found in the ethylene + α-olefin copolymerizations. In both the Zr_2 and Ti_2 catalyst systems, closer proximity of the two catalytic centers leads to significantly higher selectivities for comonomer enchainment (14, 15, 17). For Zr_2 + B_2 versus Zr_1 + B_1 catalysts under identical reaction conditions, in ethylene + 1-hexene copolymerizations, approximately three times more 1-hexene incorporation is observed, and in ethylene + 1-pentene copolymerizations, approximately four times more 1-pentene incorporation is observed. It is likely that coordination/activation of the α-olefin by a cationic metal center is stabilized by secondary, possibly agostic interactions with the proximate cationic metal center, which may facilitate/stabilize α-olefin capture/binding at the electrophilic metal center and enhance subsequent enchainment probability (Fig. 25, which is published as supporting information on the PNAS web site).

It is also found that Ti_2 in combination with the bifunctional bisborane activator BN_2 can enchain high levels of classically poorly

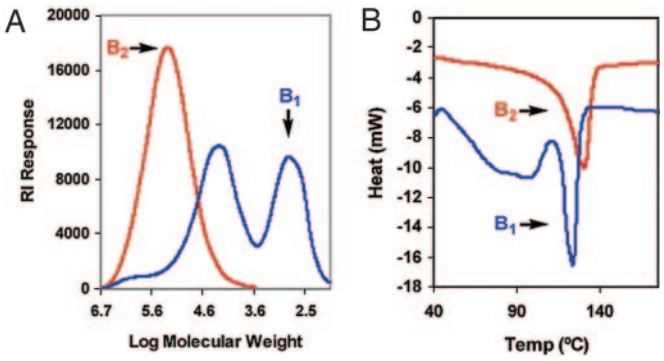

Fig. 14. Gel permeation chromatography (*A*) and differential scanning calorimetry (*B*) comparisons of polyethylenes produced by using organozirconium and organotitanium CGCs in combination with either cocatalysts B_2 or B_1.

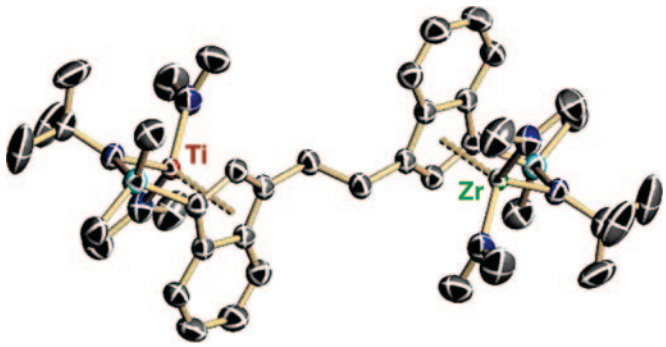

Fig. 15. Crystal structure of heterobinuclear polymerization catalyst precursor $Ti_1Zr_1(NMe_2)_4$.

responsive, sterically hindered 1,1-disubstituted comonomers such as isobutene, methylenecyclopentane, methylenecyclohexane, and 1,1,2-trisubstituted 2-methyl-2-butene in ethylene copolymerizations under mild conditions (15). For example, Ti_2 + BN_2 can enchain ≈2.3- to 5.0-times greater quantities of the above comonomers than the analogous Ti_1 + BN mononuclear catalyst under identical polymerization conditions. The copolymerizations produce novel copolymer structures: methylenecyclopentane and methylenecyclohexane are incorporated via *ring-unopened* pathways, and 2-methyl-2-butene is incorporated via a novel pathway involving comonomer isomerization to 2-methyl-1-butene followed by rapid enchainment in the copolymer backbone (Fig. 16). The effects of the ring substituents are expected to be frustration of polyolefin chain coiling and hence enhancement of the average chain length between entanglements.

Binuclear Effects in Styrene Homopolymerization and Copolymerization

The results of styrene homopolymerization/copolymerization experiments reveal striking differences between Ti_2 and Ti_1 (33). Under identical conditions, Ti_1 produces only trace quantities of styrene homopolymer, whereas Ti_2 activated by either B_1 or B_2

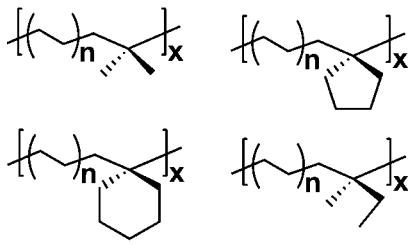

Fig. 16. Novel polyolefin copolymer structures synthesized with binuclear CGCTi-catalysts.

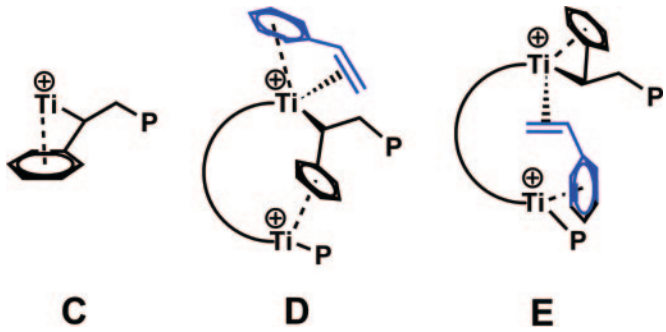

Fig. 17. Possible catalyst–arene Ti-system interactions in styrene polymerization catalysis. P = polymer.

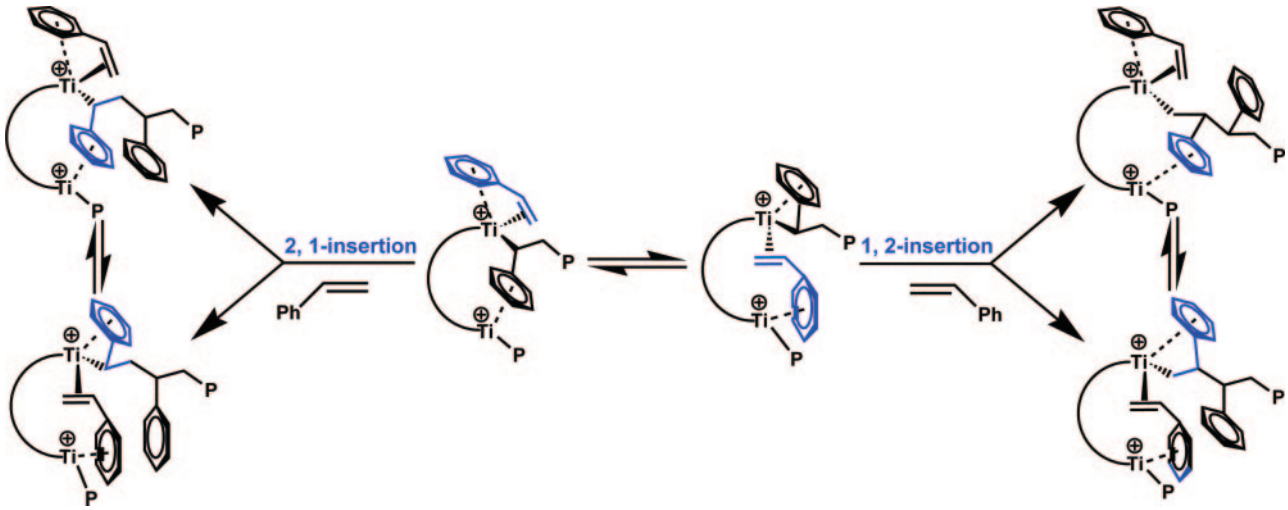

Fig. 18. Binuclear polymerization catalyst enchainment-altering interactions with styrene monomers.

exhibits significantly higher (≈50 times) homopolymerization activity. The low styrene homopolymerization activity of $\mathbf{Ti_1}$ is consistent with earlier results (34) and is thought to reflect catalytic center deactivation via intramolecular arene coordination in the 2,1-insertion product (e.g., **C**; Fig. 17) (35, 36). In contrast to this picture, for bimetallic $\mathbf{Ti_2}$, the arene ring of the last inserted styrene could preferentially coordinate to the adjacent Ti center, reducing coordinative saturation at the polymerization site and accelerating homopolymerization (37). The coordinated arene rings could in principle participate in several types of multimetallic/enchainment-altering interactions. For example, structure **D** depicts an η^n, η^2 motif in which styrene interacts with a single Ti center while the phenyl group of the last inserted styrene interacts with the second Ti (38, 39). As depicted, structure **D** would formally favor 2,1-styrene insertion, whereas structure **E** would formally favor 1,2 insertion. ^{13}C NMR end-group analysis of the homopolymer indicates that 1,2 insertion competes with 2,1 insertion to a significant degree *only in the bimetallic system*, arguing that this unusual insertion regiochemistry (40) arises from the unique catalyst nuclearity, as in Fig. 18. In ethylene + styrene copolymerizations, copolymers produced by $\mathbf{Ti_2}$ + $\mathbf{B_1}$ can have progressively higher styrene incorporation, up to 76% (Fig. 26, which is published as supporting information on the PNAS web site). When styrene incorporation is >50%, at least three consecutive head-to-tail coupled styrene units are observed in addition to tail-to-tail coupled dyads (41, 42). This result contrasts markedly with conventional mononuclear CGCs that incorporate a maximum of 50% styrene, regardless of the feed ratio, and where, of the three possible dyads, only tail-to-tail coupling is observed (34).

Conclusion and Prospects

This work has explored the degree to which the selectivity of single-site olefin polymerization processes can be modified by installing a second polymerization site (like or unlike) in close proximity to a functional site. To this end, a series of bimetallic "constrained geometry" catalysts and binuclear bisborane and bisborate cocatalysts have been synthesized and found to induce significant binuclear/cooperative enchainment effects versus their mononuclear analogs. Novel macromolecular structures and significantly improved polymer properties can be obtained by means of such binuclear catalyst/cocatalyst design strategies. It is likely that the scope of such multinuclear catalytic phenomena is quite broad and that the range of transformations that are amenable to modification by means of such cooperative effects are broader still.

We gratefully acknowledge our colleagues Drs. L. Li, N. Guo, J. Wang, G. Abramo, D. Schwartz, and M. Metz, who greatly contributed to the work described herein. We thank Profs. I. Fragala, A. Rheingold, and A. Macchioni; Drs. L. Liable-Sands, G. Lanza, A. Motta, A. Kawaoka, S. Schneider, and C. Zuccaccia; and Ms. C. Stern for enthusiastic collaboration and helpful discussions. This work was supported by Department of Energy Grant 86ER13511, National Science Foundation Grant CHE-0415407, and Dow Chemical Company.

1. Collman JP, Boulatov R, Sunderland CJ, Fu L (2004) *Chem Rev* 104: 561–588.
2. Krishnan R, Voo JK, Riordan CG, Zahkarov L, Rheingold AL (2003) *J Am Chem Soc* 125:4422–4423.
3. Bruice TC, Benkovic SJ (2000) *Biochemistry* 39:6267–6274.
4. Bruice TC (2002) *Acc Chem Res* 35:139–148.
5. Kaminsky W (2004) *J Polym Sci Polym Chem Ed* 42:3911–3921.
6. Gibson VC, Spitzmesser SK (2003) *Chem Rev* 103:283–316.
7. Gladysz JA, ed (2000) *Chem Rev* 100.
8. Marks TJ, Stevens JC, eds (1999) *Top Catal* 15.
9. Brintzinger H-H, Fischer D, Mohaupt R, Rieger B, Waymouth RM (1995) *Angew Chem Int Ed Engl* 34:1143–1170.
10. Marks TJ (1992) *Acc Chem Res* 25:57–65.
11. Chum PS, Kruper WJ, Guest MJ (2000) *Adv Mater* 12:1759–1767.
12. McKnight AL, Waymouth RM (1998) *Chem Rev* 98:2587–2598.
13. Stevens JC (1996) *Stud Surf Sci Catal* 101:11–20.
14. Li L, Metz MV, Li H, Chen M-C, Marks TJ, Liable-Sands L, Rheingold AL (2002) *J Am Chem Soc* 124:12725–12741.
15. Li H, Li L, Schwartz DJ, Metz MV, Marks TJ, Liable-Sands L, Rheingold AL (2005) *J Am Chem Soc* 127:14756–14768.
16. Li H, Li L, Marks TJ (2004) *Angew Chem Int Ed* 37:4937–4940.
17. Li H, Li L, Marks TJ, Liable-Sands L, Rheingold AL (2003) *J Am Chem Soc* 124:10788–10789.
18. Noh SK, Lee J, Lee D (2003) *J Organomet Chem* 667:53–60.
19. Wang J, Li H, Guo N, Li L, Stern CL, Marks TJ (2004) *Organometallics* 23:5112–5114.
20. Lewis SP, Henderson LD, Chandler BD, Parvez M, Piers WE, Collins S (2005) *J Am Chem Soc* 127:46–47.
21. Metz MV, Schwartz DJ, Stern CL, Marks TJ, Nickias PN (2002) *Organometallics* 21:4159–4168.
22. Williams VC, Piers WE, Clegg W, Elsegood MRJ, Collins S, Marder TB (1999) *J Am Chem Soc* 121:3244–3245.
23. Zuccaccia C, Stahl NG, Macchioni A, Chen M-C, Roberts JA, Marks TJ (2004) *J Am Chem Soc* 126:1448–1464.
24. Stahl NG, Zuccaccia C, Jensen TR, Marks TJ (2003) *J Am Chem Soc* 125:5256–5257.
25. Jin H-J, Kim S, Yoon J-S (2002) *J Appl Polym Sci* 84:1566–1571.
26. Starck P, Malmberg A, Lofgren B (2002) *J Appl Polym Sci* 83:1140–1156.
27. Komon ZJA, Bu X-H, Bazan GC (2000) *J Am Chem Soc* 122:1830–1831.
28. Komon ZJA, Diamond GM, Leclerc MK, Murphy V, Okazaki M, Bazan GC (2002) *J Am Chem Soc* 124:15280–15285.
29. Grubbs RH, Coates GW (1996) *Acc Chem Res* 29:85–93.
30. Prosenc MH, Janiak C, Brintzinger HH (1992) *Organometallics* 11:4036–4041.
31. Brookhart M, Green MLH, Wong LL (1988) *Prog Inorg Chem* 36:1–124.

32. Abramo GP, Li L, Marks TJ (2002) *J Am Chem Soc* 124:13966–13967.
33. Guo N, Li L, Marks TJ (2004) *J Am Chem Soc* 126:6542–6543.
34. Stevens JC, Timmers FJ, Wilson DR, Schmidt GF, Nickias PN, Rosen RK, Knight GW, Lai SY (1991) Eur Patent Appl 58, EP 0 416 815 A2.
35. Cotton FA, Murillo CA, Petrukhina MA (1999) *J Organomet Chem* 573:78–86.
36. Chen YX, Fu PF, Stern CL, Marks TJ (1997) *Organometallics* 16:5958–5963.
37. Nifant'ev IE, Ustynyuk LY, Besedin DV (2003) *Organometallics* 22:2619–2629.
38. Kaminsky W, Lenk S, Scholtz V, Roesky HW, Herzog A (1997) *Macromolecules* 30:7647–7650.
39. Flores JC, Wood JS, Chien JCW, Rausch MD (1996) *Organometallics* 15:4944–4950.
40. Caporaso L, Izzo L, Zappile S, Oliva L (2000) *Macromolecules* 33:7275–7282.
41. Nomura K, Okumura H, Komatsu T, Naga N (2002) *Macromolecules* 35:5388–5395.
42. Xu G, Lin S (1997) *Macromolecules* 30:685–693.